Brownmillerite-type Ca_2FeCoO_5 as a Practicable Oxygen Evolution Reaction Catalyst **

Etsushi Tsuji,*[a][b] Teruki Motohashi,*[a][c] Hiroyuki Noda,[d] Damian Kowalski,[a] Yoshitaka Aoki,[a][d] Hajime Tanida,[e]+ Junji Niikura,[e] Yukinori Koyama,[e]++ Masahiro Mori,[e]+++ Hajime Arai,[e]++++ Tsutomu Ioroi,[f] Naoko Fujiwara,[f] Yoshiharu Uchimoto,[g] Zempachi Ogumi,[e] and Hiroki Habazaki[a][d]

Abstract: Here, we report remarkable oxygen evolution reaction (OER) catalytic activity of brownmillerite (BM)-type Ca_2FeCoO_5. The OER activity of this oxide is comparable to or beyond those of the state-of-the-art perovskite (PV)-catalyst $Ba_{0.5}Sr_{0.5}Co_{0.8}Fe_{0.2}O_{3-\delta}$ (BSCF) and a precious-metal catalyst RuO_2, emphasizing the importance of the characteristic BM structure with multiple coordination environments of transition metal (TM) species. Also, Ca_2FeCoO_5 is obviously advantageous in terms of expense/laboriousness of the material synthesis. These facts make this oxide a promising OER catalyst used in many energy conversion technologies such as metal-air secondary batteries and hydrogen production from electrochemical/photocatalytic water splitting.

The oxygen evolution reaction (OER) is a key process in many energy conversion technologies. The increased demand of hydrogen fuel production has promoted the pursuit of effective OER electrocatalysts used for electrochemical/photocatalytic water splitting.[1-4] While some precious-metal catalysts such as RuO_2 (refs. 2,3) and IrO_2 (ref. 4) were found to exhibit relatively high OER catalytic activity, the scarcity of precious metals prohibits their large-scale uses. The OER is also essential for the charging process of metal-air secondary batteries which can directly convert redox energies between metallic elements and oxygen into electricity ($xM + O_2 \leftrightarrow M_xO_2$; M = Li, Zn, etc.). This technology is suitable for energy storage devices in next generation electric vehicles, and cost-effective TM-based catalysts incorporated therein have attracted increased attention. However, the lack of highly active and durable air electrode catalysts is an obstacle to realize batteries with sufficient charge-discharge efficiency and lifetime.[5-9] Nano-materialization of NiFe-based compounds including alloys, oxides, and hydroxides have been studied to improve the OER catalytic activity and long-term durability.[8,10-12] Meanwhile, the exploration of novel catalysts for OER as well as the oxygen reduction reaction (ORR) have been eagerly carried out among compounds that are industrially producible in large scales, such as the PV-type oxide family (ABO_3).[13-17]

To gain a systematic understanding of the OER activity of PV oxides, various dominating factors were studied both from the electronic and crystallographic points of view. Suntivich et al. have proposed an e_g occupancy at the B site as a simple descriptor, that is, the OER activity tends to be high when the e_g electron number is close to unity.[14] Based on this strategy,

[a] Dr. E. Tsuji, Dr. T. Motohashi, Dr. D. Kowalski, Dr. Y. Aoki, Dr. H. Habazaki
Division of Applied Chemistry, Hokkaido University
Sapporo 060-8628 (Japan)
[b] Dr. E. Tsuji
Department of Chemistry and Biotechnology, Tottori University
Tottori 680-8550 (Japan)
E-mail: e-tsuji@chem.tottori-u.ac.jp
[c] Dr. T. Motohashi
Department of Materials and Life Chemistry, Kanagawa University
Yokohama 221-8686 (Japan)
E-mail: t-mot@kanagawa-u.ac.jp
[d] Mr. Y. Noda, Dr. Y. Aoki, Dr. H. Habazaki
Graduate School of Chemical Sciences and Engineering, Hokkaido University
Sapporo 060-8628 (Japan)
[e] Dr. H. Tanida, Mr. J. Niikura, Dr. Y. Koyama, Dr. M. Mori, Dr. H. Arai, Dr, Z. Ogumi
Office of Society-Academia Collaboration for Innovation, Kyoto University
Kyoto 611-0011 (Japan)
[f] Dr. T. Ioroi, Dr. N. Fujiwara
National Institute of Advanced Industrial Science and Technology
Osaka 563-8577 (Japan)
[g] Dr. Y. Uchimoto
Graduate School of Human and Environmental Studies, Kyoto University
Kyoto 606-8501 (Japan)
[+] Present address:
Battery Analysis Laboratory, Device Analysis Department, NISSAN ARC, LTD.
Kanagawa 237-0061 (Japan)
[++] Present address:
Center for Materials Research by Information Integration (CMI^2), Research and Services Division of Materials Data and Integrated System (MaDIS), National Institute for Materials Science (NIMS)
Ibaraki 305-0047 (Japan)
[+++] Present address:
Materials science research group, Research institute of electrochemical energy, Department of energy and environment, National institute of advanced industrial science and technology (AIST)
Osaka 563-8577 (Japan)
[++++] Present address:
School of Materials and Chemical Technology, Tokyo Institute of Technology
Yokohama 226-8502 (Japan)

Supporting information for this article is given via a link at the end of the document.

[**] This work was supported by the RISING (Research and Development Initiative for Science Innovation of New Generation Batteries) and RISING2 projects of the New Energy and Industrial Technology Development Organization (NEDO), Japan. The synchrotron radiation experiments were performed with the approval of the Japan Synchrotron Radiation Research Institute (JASRI; Proposal Nos. 2014B7600 and 2015A7600). A part of this work was conducted at "Joint-use Facilities: Laboratory of Nano-Micro Material Analysis", Hokkaido University, supported by "Nanotechnology Platform" Program of the Ministry of Education, Culture, Sports, Science and Technology (MEXT), Japan.

they found high OER activity in a cobalt/iron oxide BSCF containing $Co^{2.8+}$ (intermediate-spin; $t_{2g}^5e_g^{1.2}$).[15-17] Meanwhile, it has been suggested that the presence of oxygen deficiencies also plays an important role in promoting OER.[17-21] In this regard, highly oxygen-deficient PVs may be potential OER catalysts, as a large number of oxygen deficiencies should act as adsorption/reaction centers for hydroxide anions in alkaline media. We thus focused on TM oxides with a BM-type structure, generally formulated with $A_2B_2O_5$. The BM structure is categorized as an oxygen-deficiency-ordered PV containing a layered arrangement of tetrahedral (*Td*) BO_4 and octahedral (*Oh*) BO_6, as illustrated in Figure 1a. This structure is noteworthy because of its highest density of oxygen deficiencies among stable PV-derived lattices. BM-type oxides were previously investigated focusing on their crystallography,[22,23] magnetism,[24] ionic conductivity,[25] catalytic activity to produce carbon nanotubes,[26] and oxygen storage capability.[27] While BM-type $SrCoO_{2.5}$ was reported to exhibit ORR activity at 500 – 600 °C,[28] extensive researches on BM-type OER electrocatalysts have never been conducted. From our recent survey on this "unexplored" oxide family, a significantly high OER activity was revealed for Ca_2FeCoO_5 (CFCO).

The OER activity of BM-type CFCO is compared with those of an isoelectronic PV-type $LaFe_{0.5}Co_{0.5}O_3$ (LFCO) together with BSCF and RuO_2 (Figure 1c). The CFCO sample, synthesized by a conventional solid-state reaction at 1100 °C (denoted "S1100"), exhibits a large anodic current in a 4 mol dm^{-3} KOH aqueous solution despite its small specific surface area (< 1 m^2 g^{-1}, see Table S1). The OER current density of CFCO normalized with the specific surface area is an order of magnitude larger than those of the reference catalysts at 1.60 V vs reversible hydrogen electrode (RHE). Also noticeably, the onset potential of OER current clearly shifts to a negative direction. The overpotential (η) vs current density (J) relation presented in Figure 1d nicely follows the Tafel equation for all the catalysts showing similar slopes as large as 60 mV dec^{-1} (Log J vs η curves in a wider range are presented in Figure S1). The value of the Tafel slope is comparable to those of PV catalysts reported in the previous literature.[14,30] While the OER activity of our reference catalysts is somewhat lower than that reported in the literature,[14] the OER activity of CFCO is beyond those of LFCO and even the state-of-the-art PV catalyst BSCF in the experimental condition employed in the present work. The OER property of CFCO is obviously unusual and hard to be explained only within the aforementioned molecular orbital principles proposed by Suntivich et al.[14]

Another superiority of the CFCO catalyst comes from its chemical constituent. The fact that CFCO consists largely of ubiquitous elements makes this oxide a promising material for large-scale practical uses. Surely even cobalt is regarded as a rare metal, but its price is several orders of magnitude lower than that of ruthenium or iridium. It should also be noted that this oxide does not contain barium and strontium but only calcium as alkali-earth constituents. Calcium-based oxides are favorable, not only in terms of the raw material expense, but also when aiming for the enhanced surface area by lowering synthesis temperature. Since calcium carbonate is thermally less stable than the barium and strontium counterparts,[31] phase-pure CFCO products were successfully obtained via a wet-chemical route even with firing temperatures as low as 600 - 800 °C (Figure S2). This feature is in contrast to the case of BSCF, for which sample syntheses below 900 °C were unsuccessful due to poor reactivity of $BaCO_3$ in the precursor material. The resultant CFCO products indeed contain submicron-sized fine grains (Figure S3) with larger specific surface areas of > 15 m^2 g^{-1}. Recent extensive surveys by other groups also revealed some potential PV catalysts such as $PrBaCo_2O_{5+\delta}$ (ref. 30), $SrNb_{0.1}Co_{0.7}Fe_{0.2}O_{3-\delta}$ (ref. 32), $SrCo_{0.9}Ti_{0.1}O_{3-\delta}$ (ref. 33), $BaCo_{0.7}Fe_{0.1}Sn_{0.2}O_{3-\delta}$ (ref. 34) and $CaCu_3Fe_4O_{12}$ (ref. 35). Nevertheless, these materials need relatively high synthesis temperatures (≥ 1000 °C) because of poor reactivity of the chemical reagents and/or their complicated cationic arrangement ($CaCu_3Fe_4O_{12}$ also requires ultra-high pressures). Consequently, the specific surface area of the products is inevitably reduced, resulting in insufficient OER current values in actual operations. On the other hand, the CFCO fine powders synthesized at 600 and 800 °C (denoted "W600" and "W800", respectively) exhibit significantly improved OER performance when normalized by the catalyst quantity (the OER current density and the Tafel slope of CFCO_W800 normalized by the specific surface area are almost the same as those of CFCO_S1100 in Figures 1c and 1d). As demonstrated in Figure 1e, the OER current density per disc- electrode area reaches 100 mA cm^{-2}_{disc} at 1.50 V vs RHE for the W600 powder. In fact, the OER current density values of the CFCO fine powders come close to those reported for highly sophisticated NiFe-based material/carbon nanocomposites.[10-12]

Let us discuss the origin of the remarkable OER property of CFCO. A previous neutron scattering study on this oxide revealed that iron and cobalt are distributed homogeneously both in the *Td* and *Oh* layers.[36] Previous X-ray absorption near edge structure (XANES) studies indicated that Fe and Co are trivalent,[37] in good agreement with the XANES data in the present work (Figure S4). This implies that Fe/Co species within the *Oh* layer are essentially identical to those in the PV catalysts. To gain deeper insight into the role of Fe/Co in the OER activity, the BM-type $Ca_2Fe_{2-x}Co_xO_5$ system was synthesized and characterized in the range of $0 \le x \le 1.0$ (sample syntheses for $x > 1.0$ were unsuccessful; for XRD patterns and SEM images, see Figures S5 and S6, respectively). As presented in Figure 2, all the $Ca_2Fe_{2-x}Co_xO_5$ samples exhibit relatively high OER activity, indicative of a structural advantage of the BM lattice. The data also reveal that the magnitude of OER current systematically increases with the increasing Co content (x). In addition, the electrical conductivity is found to be enhanced in Co-rich x = 0.75 and 1.0 samples (Figure S7), consistent with the report of Cascos et al.[38] Thus, the remarkable OER activity of CFCO can be explained partly by its improved electrical conductivity. Meanwhile, a closer look at the OER data highlights a characteristic behavior with regard to cobalt substitution: the overpotential to give a current density of 10 μA cm^{-2}_{oxide} linearly decreases up to x = 0.50 and tends to be constant at $x \ge 0.50$.

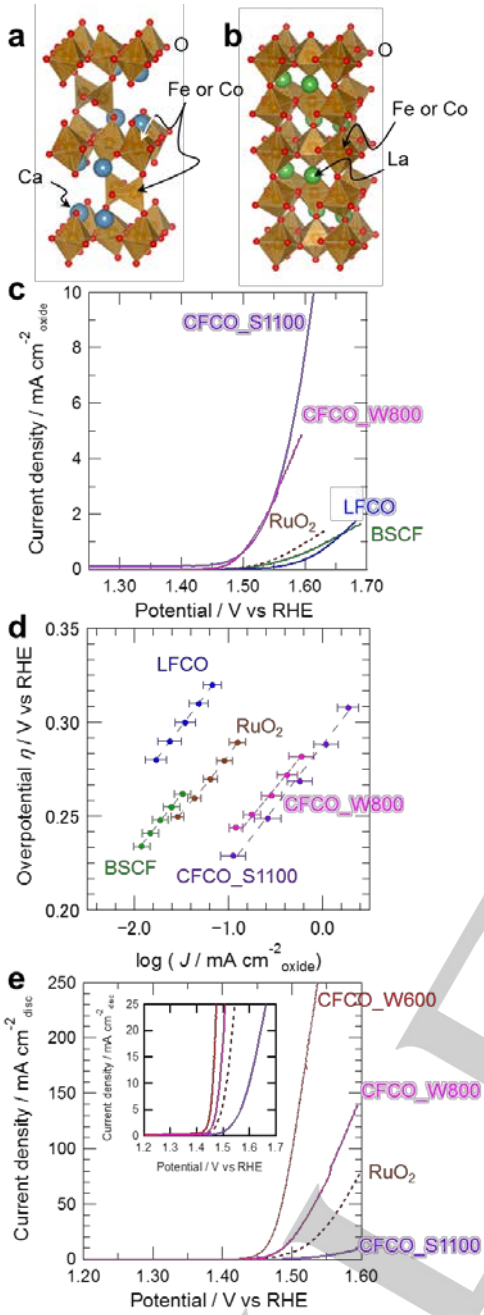

Figure 1. (a) Crystal structures of BM-type Ca_2FeCoO_5 (CFCO) and (b) its isoelectronic reference oxide, PV-type $LaFe_{0.5}Co_{0.5}O_3$ (LFCO). The illustrations were drawn with VESTA software[29] based on the structural model reported in the literature. (c) Linear sweep voltammograms of CFCO_S1100, W800, LFCO, BSCF and RuO_2 for OER. The current density was normalized with the specific surface areas. (d) Tafel plots of CFCO_S1100, W800, LFCO, BSCF and RuO_2. Error bars represent standard deviations from at least four independent measurements. (e) Linear sweep voltammograms of CFCO_S1100, W800, W600, and RuO_2. The current density was normalized with the geometric surface area of the disc electrode. All the measurements were conducted at room temperature in a 4 mol dm^{-3} KOH aqueous solution. It should be emphasized that the usage of concentrated alkaline solutions is mandatory for constructing practical metal-air secondary batteries to enhance the ionic conductivity of the electrolyte and to suppress corrosions of the negative electrodes. Such OER data with high KOH concentrations are thus informative to evaluate the performance in practical metal-air secondary batteries.

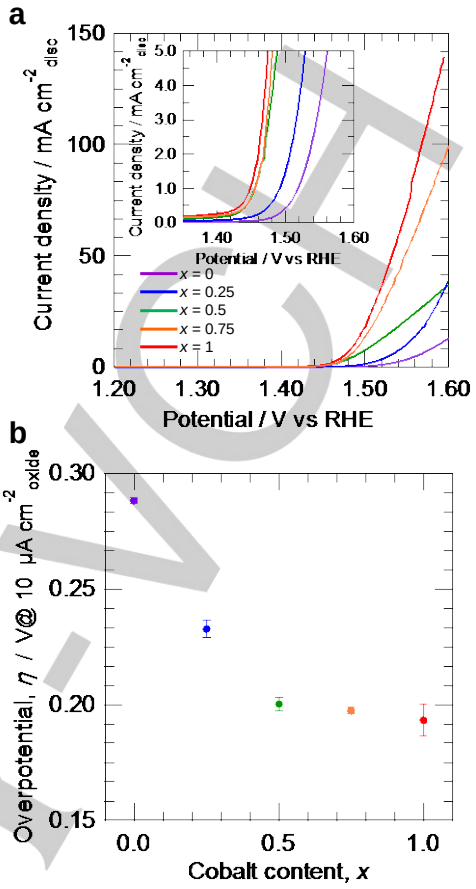

Figure 2. (a) Linear sweep voltammograms of $Ca_2Fe_{2-x}Co_xO_5$ ($0 \le x \le 1$) for OER. The samples were synthesized via a wet-chemical route with a firing temperature of 800 °C. The current density was normalized with the geometric surface area of the disc electrode. (b) The overpotentials (η) vs cobalt content (x) relation for $Ca_2Fe_{2-x}Co_xO_5$ ($0 \le x \le 1$). The η values were determined from the onset potential E_{onset}; E_{onset} is the potential to give a current density, which was normalized with the specific surface areas (Table S2), of 10 μA cm^{-2}_{oxide}.

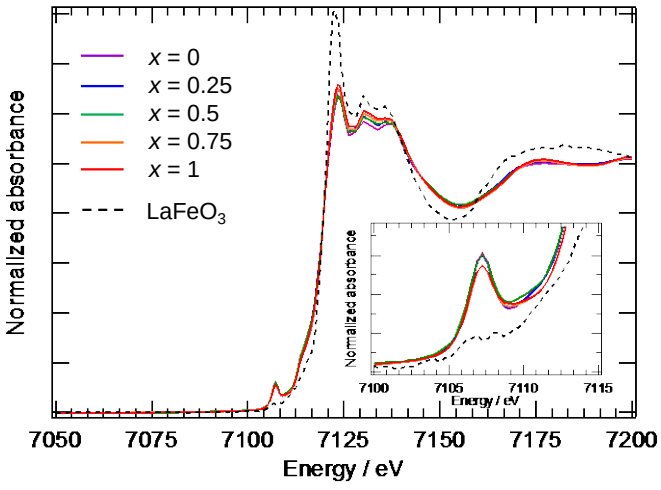

Figure 3. Fe *K*-edge XANES spectra of $Ca_2Fe_{2-x}Co_xO_5$ and $LaFeO_3$. The inset represents enlarged spectra in the vicinity of the pre-edge peak attributable to *Td*-Fe in $Ca_2Fe_{2-x}Co_xO_5$.

Table 1. Relative intensity values of the pre-edge peak for the $Ca_2Fe_{2-x}Co_xO_5$ samples.

x in $Ca_2Fe_{2-x}Co_xO_5$	Relative peak intensity
0	1.0
0.25	0.97
0.50	0.98
0.75	0.89
1.0	0.89

This behavior would be related to the selective site occupancy of cobalt in the BM lattice. Figure 3 shows Fe *K*-edge XANES spectra of the $Ca_2Fe_{2-x}Co_xO_5$ samples. As indicated by the inset of the figure and Table 1, the relative intensity of the pre-edge peak attributable to *Td*-Fe[39] is nearly constant for cobalt contents up to $x = 0.50$, and then starts to decrease upon further substitution. This implies that cobalt preferentially substitutes iron in the *Oh* layer for small substitution levels, and then in the *Td* layer at $x \geq 0.50$. Such a site preference is supported by the energy diagram of the $Ca_2Fe_{2-x}Co_xO_5$ system obtained by density functional calculations, see Figure S8. Unfortunately, we were unable to accurately estimate the cobalt occupancy at each site, because the Co *K*-edge is overlapped with the extended region of the Fe *K*-edge.

Taking into account the experimental fact that the OER current is enhanced remarkably at $x \geq 0.50$, *Td*-Co species are assumed to provide additional reaction sites to enhance the turnover frequency. Besides, the *Oh*-Co may contribute to catalyzing the electron transfer from the reactants (= hydroxide anions) to the catalyst, on the basis of the molecular orbital principles.[14] That is to say, the *Oh*- and *Td*-sites are likely to play distinct roles in the enhanced OER activity: the former mainly lowers the overpotential, and the latter enhances the OER current. In fact, the OER activity of CFCO is less prominent when compared in a diluted KOH aqueous solution, as demonstrated in Figure S9 of the Supporting Information. That is, CFCO exhibits strongly pH-dependent OER property, suggesting that the adsorption of hydroxide anions is a key factor. We emphasize that the OER activity of CFCO may not be explained only within the already-established design principle of high-performance catalysts, and our model needs to be verified employing the molecular orbital theory.

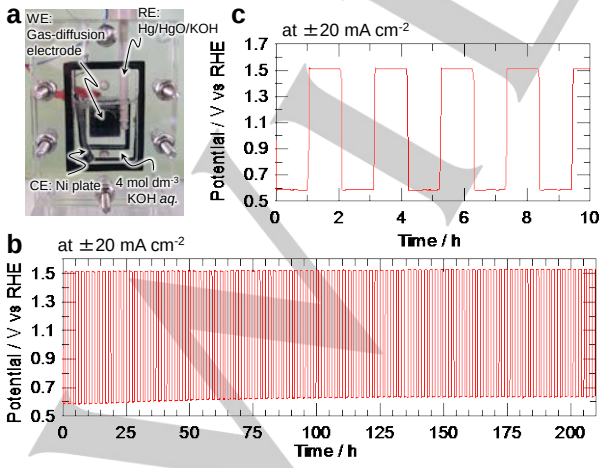

Figure 4. (a) A photograph of the test cell used for the cyclic durability test of the CFCO gas-diffusion electrode. (b) ORR/OER cycles of the CFCO electrode at a current density of 20 mA $cm^{-2}_{electrode}$ positively/negatively switched in every hour. (c) The enlarged plot in the initial stage at a period of 0 - 10 h.

Finally, we demonstrate that CFCO exhibits superior structural and chemical stabilities against prolonged/repeated electrochemical cycles. To check the durability under an OER condition, a constant potential of 1.7 V vs RHE was applied to the W800 catalyst for 8 h, see Figure S10. It is noteworthy that the current density is nearly constant during the OER test, and linear sweep voltammograms are essentially identical before and after the application of the constant potential, strongly suggesting that any structural modifications can be ruled out. The inductively coupled plasma-atomic emission spectrometry (ICP-AES) analysis on the catalyst revealed negligible amounts of constituent elements dissolved in the electrolyte even after the OER test (Table S3). This behavior is in sharp contrast to the result of BSCF,[17] where its voltammograms are unstable during the repeating electrochemical cycles, which is attributed to grain-surface amorphization in the early stage of OER. We note that the actual nature of the grain surface should largely influence the catalytic activity. The chemical composition and adsorbed nature of the outermost surface are still unclear and merit further investigations.

Then, a cyclic durability under alternating current flow was also tested employing a practical half-cell geometry of metal-air secondary batteries. A gas-diffusion electrode of the W600 fine powder was fabricated and its voltage polarization was measured at a current density of 20 mA $cm^{-2}_{electrode}$ positively/negatively switched in every an hour. As presented in Figure 4, the potential of the CFCO electrode immediately increases and reaches a stable value at 1.51 V vs RHE when a positive current is applied, and remarkably, no increase in the OER potential is observed even after 200 hours of total duration (100 cycles of OER/ORR). It should be noted that no sign of degradation is found also in the ORR process. We suggest that the excellent cyclic durability of CFCO is attributed to the chemical stability of the stoichiometric BM lattice, as revealed by thermogravimetric analyses under oxidative/ reductive atmospheres (see Figure S11).

In summary, BM-type CFCO was found to exhibit remarkable OER catalytic activity. This oxide may be regarded as a promising catalyst for practical OER applications from every standpoint of catalytic performance, economic/ productive efficiencies, and long-term durability. Our systematic study on the $Ca_2Fe_{2-x}Co_xO_5$ solid solution suggests that the combination of *Td*/*Oh*-sites in the BM structure plays a crucial role. The present work highlights a novel functionality of the BM oxide family, in which multiple coordination environments are believed to give synergetic effects.

Experimental Section

Synthesis. The CFCO samples were synthesized by a solid-state reaction at 1100 °C (denoted "S1100") or via a wet-chemical route with firing temperatures of 600 and 800 °C ("W600" and "W800", respectively). LFCO and BSCF were synthesized similarly via the wet-chemical route.

Details of other experimental procedures can be found in the Supporting Information.

Keywords: electrocatalysts • oxygen evolution reaction • brownmillerite-type oxides

[1] A. Fujishima, K. Honda, *Nature* **1972**, *237*, 37-38.
[2] E. Tsuji, A. Imanishi, K. Fukui, Y. Nakato, *Electrochim. Acta* **2011**, *56*, 2009-2016.
[3] N. Danilovic, R. Subbaraman, K. C. Chang, S. H. Chang, Y. J. Kang, J. Snyder, A. P. Paulikas, D. Strmcnik, Y. T. Kim, D. Myers, V. R. Stamenkovc, N. M. Markovic, *J. Phys. Chem. Lett.* **2014**, *5*, 2474-2478.
[4] M. Yagi, E. Tomita, T. Kuwabara, *J. Electroanal. Chem.* **2005**, *579*, 83-88.
[5] F. Cheng, J. Chen, *Chem. Soc. Rev.* **2012**, *41*, 2172-2192.
[6] Z. L. Wang, D. Xu, J. J. Xu, X. B. Zhang, *Chem. Soc. Rev.* **2014**, *43*, 7746-7786.
[7] D. U. Lee, P. Xu, Z. P. Cano, A. G. Kashkooli, M. G. Park, Z. Chen, *J. Mater. Chem. A* **2016**, *4*, 7107-7134.
[8] Y. Li, H. Dai, *Chem. Soc. Rev.* **2014**, *43*, 5257-5275.
[9] W. Wang, X. Xu, W. Zhou, Z. Shao, *Adv. Sci.* **2017**, *4*, 1600371.
[10] M. Gong, H. Dai, *Nano Research* **2015**, *8*, 23-39.
[11] Y. Li, M. Gong, Y. Liang, J.-E. Kim, H. Wang, G. Hong, B. Zhang, H. Dai, *Nat. Commun.* **2013**, *4*, 1805.
[12] Y. Feng, H. Zhang, Y. Zhang, X. Li, Y. Wang, *ACS Appl. Mater. Interfaces* **2015**, *7*, 9203-9210.
[13] C. K. Lee, K. A. Striebel, F. R. McLarnon, E. J. Cairns, *J. Electrochem. Soc.* **1997**, *144*, 3801-3806.
[14] J. Suntivich, K. J. May, H. A. Gasteiger, J. B. Goodenough, Y. S. Horn, *Science* **2011**, *334*, 1383-1385.
[15] C. Jin, X. Cao, F. Lu, Z. Yang, R. Yang, *Int. J. Hydrogen Energy* **2013**, *38*, 10389-10393.
[16] M. Risch, A. Stoerziger, S. Maruyama, W. T. Hong, I. Takeuchi, Y. S. Horn, *J. Am. Chem. Soc.* **2014**, *316*, 5229-5232.
[17] K. J. May, C. E. Carlton, K. A. Stoerzinger, M. Risch, J. Suntivich, Y. L. Lee, A. Grimaud, Y. S. Horn, *J. Phys. Chem. Lett.* **2012**, *3*, 3264-3270.
[18] R. Gao, L. Liu, Z. Hu, P. Zhang, X. Cao, B. Wang, X. Liu, *J. Mater., Chem., A* **2015**, *3*, 17598-17605.
[19] C. F. Chen, G. King, R. M. Dickerson, P. A. Papin, S. Gupta, W. R. Kellogg, G. Wu, *Nano Energy* **2015**, *13*, 423-432.
[20] A. Ramírez, P. Hillebrand, D. Stellmach, M. M. May, P. Bogdanoff, S. Fiechter, *J. Phys. Chem. C* **2014**, *118*, 14073-14081.
[21] J. R. Petrie, H. Jeen, S. C. Barron, T. L. Meyer, H. N. Lee, *J. Am. Chem. Soc.* **2016**, *138*, 7252-7255.
[22] E. V. Antipov, A. M. Abakumov, S. Y. Lstomin, *Inorg. Chem.* **2008**, *47*, 8543-8552.
[23] A. Nemudry, M. Weiss, I. Gainutdinov, V. Boldyrev, R. Schöllhorn, *Chem. Mater.* **1998**, *10*, 2403-2411.
[24] T. Takeda, Y. Yamaguchi, S. Tomiyoshi, M. Fukase, M. Sugimoto, H. Watanabe, *J. Phys. Soc. Jpn.* **1968**, *24*, 446-452.
[25] K. R. Kendall, C. Navas, J. K. Thomas, H. C. Loye, *Solid State Ionics* **1995**, *82*, 215-223.
[26] N. Chiwaye, L. L. Jewell, D. G. Billing, D. Naidoo, M. Ncube, N. J. Coville, *Mater. Res. Bull.* **2014**, *56*, 98-106.
[27] T. Motohashi, Y. Hirano, Y. Masubuchi, K. Oshima, T. Setoyama, S. Kikkawa, *Chem. Mater.* **2013**, *25*, 372-377.
[28] H. Jeen, Z. Bi, W. S. Choi, M. F. Chisholm, C. A. Bridges, M. P. Paranthaman, H. N. Lee, *Adv. Mater.* **2013**, *25*, 6459-6463.
[29] K. Momma, F. Izumi, *J. Appl. Crystallogr.* **2011**, *44*, 1272-1276.
[30] A. Grimaud, K. J. May, C. E. Carlton, Y. L. Lee, M. Risch, W. T. Hong, J. Zhou, Y. S. Horn, *Nat. Commun.* **2013**, *4*, 2439.
[31] J. M. Criado, M. J. Diánez, *J. Mater. Sci.* **2004**, *39*, 5189-5193.
[32] Y. Zhu, W. Zhou, Z. G. Chen, Y. Chen, C. Su, M. O. Tadé, Z. Shao, *Angew. Chem. Int. Ed.* **2015**, *54*, 3897-3901.
[33] C. Su, W. Wang, Y. Chen, G. Yang, X. Xu, M. O. Tadé, Z. Shao, *ACS Appl. Mater. Interfaces* **2015**, *7*, 17663-17670.
[34] X. Xu, C. Su, W. Zhou, Y. Zhu, Y. Chen, Z. Shao, *Adv. Sci.* **2016**, *3*, 1500187.
[35] S. Yagi, I. Yamada, H. Tsukasaki, A. Seno, M. Murakami, H. Fujii, H. Chen, N.Umezawa, H. Abe, N. Nishiyama, S. Mori, *Nat. Commun.* **2015**, *6*, 8249.
[36] F. Ramezanipour J. E. Greedan, A. P. Grosvenor, J. F. Britten, L. M. D. Cranswick, V. O. Garlea, *Chem. Mater.* **22**, 6008-6020 (2010).
[37] A. P. Grosvenor, J. E. Greedan, *J. Phys. Chem. C* **2009**, *113*, 11366-11372.
[38] V. Cascos, R. Martínez-Corronada, J. A. Alonso, M. T. Fernández-Díaz, *Int. J. Hydrogen Energy* **2015**, *40*, 5456-5468.
[39] A. L. Roe, D. J. Schneider, R. J. Mayer, J. W. Pyrz, J. Widom, L. Que, Jr., *J. Am. Chem. Soc.* **1984**, *106*, 1676-1681.

Entry for the Table of Contents (Please choose one layout)

COMMUNICATION

Text for Table of Contents

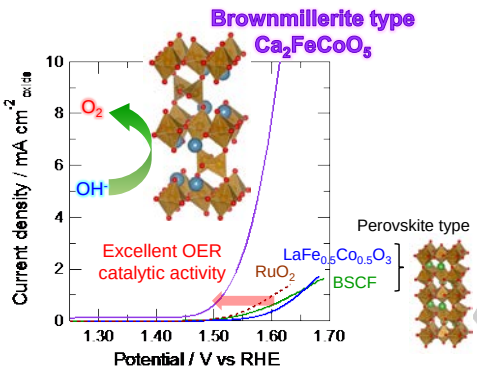

Etsushi Tsuji, Teruki Motohashi,* Hiroyuki Noda, Damian Kowalski, Yoshitaka Aoki, Hajime Tanida, Junji Niikura, Yukinori Koyama, Masahiro Mori, Hajime Arai, Tsutomu Ioroi, Naoko Fujiwara, Yoshiharu Uchimoto, Zempachi Ogumi, and Hiroki Habazaki*

Page No. – Page No.
Brownmillerite-type Ca_2FeCoO_5 as a Practicable Oxygen Evolution Reaction Catalyst